



Fluid transport in high volume fly ash mixtures with and without internal curing



Igor De la Varga^{a,*}, Robert P. Spragg^b, Carmelo Di Bella^c, Javier Castro^d, Dale P. Bentz^e, Jason Weiss^b

^a SES Group & Associates LCC, Turner-Fairbank Highway Research Center, Federal Highway Administration, 6300 Georgetown Pike, McLean, VA 22101, USA

^b School of Civil Engineering, Purdue University, West Lafayette, IN, USA

^c EMPA – Swiss Federal Laboratories for Materials Science and Technology, Dübendorf, Switzerland

^d Faculty of Engineering, Universidad del Desarrollo, Santiago, Chile

^e National Institute of Standards and Technology (NIST), Gaithersburg, MD, USA

ARTICLE INFO

Article history:

Received 13 May 2013

Received in revised form 27 August 2013

Accepted 15 September 2013

Available online 28 September 2013

Keywords:

Transport properties

High volume fly ash

Internal curing

Chloride

Water absorption

ABSTRACT

The transport of fluid and ions in concrete mixtures is central to many aspects of concrete deterioration. As a result, transport properties are frequently measured as an indication of the durability that a concrete mixture may be expected to have. This paper is the second in a series investigating the performance of high volume fly ash (HVFA) mixtures with low water-to-cementitious ratios (w/cm) that are internally cured. While the first paper focused on strength and shrinkage, this paper presents the evaluation of the transport properties of these mixtures. Specifically, the paper presents results from: rapid chloride migration (RCM), rapid chloride penetration test (RCPT), apparent chloride diffusion coefficient, surface electrical resistivity, and water absorption. The test matrix consisted of mortar samples with two levels of class C fly ash replacement (40% and 60% by volume) with and without internal curing provided with pre-wetted lightweight fine aggregates (LWA). These mixtures are compared to plain ordinary portland cement (OPC) mortars. The results indicate that HVFA mixtures with and without internal curing provide benefits in terms of reduced transport coefficients compared to the OPC mixtures.

© 2013 Elsevier Ltd. All rights reserved.

1. Introduction

Fly ash is a by-product of coal combustion in power plants that can be used in concrete as a cement replacement [1]. The replacement of cement with fly ash can contribute positively in improving the sustainability of the concrete construction industry in a number of ways: (1) using less cement so that the clinker factor per cubic yard of concrete is reduced, (2) using a waste product (fly ash) that no longer needs to be landfilled, and (3) improving properties affecting the durability of concrete. The amount of fly ash replacement for cement that is typically used in concrete pavements and transportation structures is limited by specifications to approximately 20–25% by mass, due to strength and de-icer scaling concerns [2]. High volume fly ash (HVFA) concrete mixtures where cement replacement is increased to be on the order of 50% or more have demonstrated the potential to perform very well or achieve specific characteristics in a series of studies [3]. For example, the use of HVFA in mass concrete applications can reduce the heat of hydration and resulting thermal effects [4], thereby minimizing early-age cracking.

Concerns with the use of HVFA are related to slow rate of hydration which can result in slow strength gain and extended curing times. To overcome these limitations, the research team has taken an approach that can be used to offset the slow strength development of HVFA mixtures [5]. This approach consists of reducing the water-to-cementitious materials mass ratio (w/cm). However, as the w/cm is reduced, increased autogenous shrinkage is typically observed [6]. In addition, the low w/cm concrete mixtures may become more difficult to water cure, as the curing water can only penetrate a few millimeters due to the much denser microstructure that forms [7]. This issue of self-desiccation in high performance concrete has been discussed by Philleo [8]. Internal curing (IC) has been developed as one potential approach to improve curing and to distribute curing water throughout the concrete's cross section. IC consists of mixing in pre-wetted porous lightweight aggregates (LWA) that act as water reservoirs within the concrete, and subsequently exploiting the mechanism of chemical shrinkage to draw water from the LWA to the paste as needed during hydration, thereby curing the concrete from within [7].

The use of HVFA mixtures with a low w/cm may be expected to improve performance in terms of reduced transport properties (i.e., water and ion penetrability). Transport properties depend on total porosity, pore size distribution, pore connectivity, and pore tortuosity [9]. Internal curing elevates the rate of hydration at later ages,

* Corresponding author. Tel.: +1 202 493 3433.

E-mail address: igor.delavarga.ctr@dot.gov (I. De la Varga).

which refines the pore structure and reduces the transport of water and ions through the cement matrix at a given age [10]. Bentz [11] suggested that the quality of the interfacial transition zone (ITZ) is another factor to consider in transport performance when comparing mixtures with and without IC, but to a lesser degree than the pore tortuosity of the bulk matrix [12]. It has been shown that IC improves the quality of the ITZ [13,14], which also reduces transport.

This paper presents a series of tests that highlight the transport properties of HVFA mixtures with IC, following up on an initial study that focused on mechanical properties, shrinkage, and early-age cracking [5].

2. Materials and mixture proportions

As previously mentioned, this paper considers an approach to use a HVFA mixture as a potential substitute for a typical concrete mixture design. For example, a conventional pavement mixture design in the state of Indiana would consist of a water-to-cement ratio, $w/c = 0.42$ to achieve specific performance requirements, including early-age strength. To use higher volumes of fly ash, the w/c (w/cm) has to be reduced to compensate for the otherwise low early age strength. As a result, a $w/c = 0.30$ was used with 40% and 60% replacement by volume of cement with fly ash. The testing matrix consisted of six mixtures. Two plain mortar mixtures were prepared using ordinary portland cement ($w/c = 0.30$; $w/c = 0.42$). Two HVFA mortars were prepared with w/c of 0.30 with 40% and 60% of the cement replaced with fly ash (by volume). These two HVFA mortar mixtures were also prepared with pre-soaked LWA for internal curing. The mixture proportions of the mortars are summarized in Table 1. The mixture with a w/c of 0.42 would correspond to a typical mixture design used in transportation structures (e.g., bridge deck). In Table 1, “L” stands for LWA and identifies the internally-cured mortars.

An ordinary portland cement (OPC), ASTM C150-09 Type I/II, was used in this study, with a Blaine fineness of $476 \text{ m}^2/\text{kg}$, a density of $3170 \text{ kg/m}^3 \pm 10 \text{ kg/m}^3$, an estimated Bogue potential phase composition of 52% C_3S , 18% C_2S , 8% C_3A , and 9% C_4AF by mass, and a Na_2O equivalent of 0.5% by mass. A Class C fly ash (ASTM C618-08a) was also used with a density of $2630 \text{ kg/m}^3 \pm 10 \text{ kg/m}^3$. The fine aggregate used was ordinary river sand with a fineness modulus of 2.71 and an apparent specific gravity of 2.58. Rotary kiln expanded shale (i.e., a lightweight fine aggregate) was used with a fineness modulus of 3.97 and an oven dry specific gravity of 1.38. The lightweight aggregate (LWA) was measured to have a 24 h water absorption of 17.5% by dry mass, when this material was tested using the paper towel technique [15,16]. A polycarboxylate-based high-range water-reducing admixture (HRWRA) was added at variable dosage by mass of cement in order to maintain

the same (mini) slump in all mortars [17]. While the fly ash replacement for cement was performed on a volumetric basis, the w/cm of the last five mortars was maintained constant on a mass basis (following current industry practice), implying that these mixtures have variable initial capillary porosities.

In this study, sealed curing conditions were used for many of the mortar specimens, both those with and without IC. These curing conditions were selected as providing the most representative match for the curing that would be experienced by the interior of a concrete member in the field [18]. To proportion the internally cured mixtures a methodology is used that is based on a procedure developed by Bentz, and reported in Bentz et al. [7], in which the amount of LWA is calculated based on the chemical shrinkage occurring in the sample. In this study, a chemical shrinkage value of 6.4% was assumed for all the internally cured mixtures.

3. Test methods

A series of tests were performed to assess the transport properties of the plain, HVFA, and internally cured HVFA mixtures. A total of five different tests methods were used. The tests are divided into 3 main groups. The first set of tests (3.1–3.3) is related with the movement (i.e., diffusion) of chloride ions in concrete. The second test (3.4) describes the electrical properties (e.g., surface resistivity) of the mixtures. Finally, the third test (3.5) describes water absorption (ASTM C1585).

3.1. Rapid chloride migration – NT Build 492

The rapid chloride migration test (RCM) was conducted to determine the non-steady state chloride migration coefficients following the NT Build 492 procedure [19,20]. The RCM test accelerates the chloride transport by applying an electrical potential across the specimen for a specified period of time. The test samples were prepared from cylinders with a diameter of 102 mm [4 in.] and length of 204 mm [8 in.]. The day after casting, the samples were demolded, sealed in double plastic bags and stored at $(23 \pm 0.5)^\circ\text{C}$ [$(73.4 \pm 0.8)^\circ\text{F}$] until the age of testing was reached. The reason for this is that the IC effects are better observed in sealed-cured samples rather than in moist-cured samples. Additionally, as mentioned above, sealed-curing provides the most representative match for the curing that would be experienced by the interior of a concrete member in the field [18]. The cylinders were cut into disks having a length of $(51 \pm 2) \text{ mm}$ [$(2 \pm 0.08) \text{ in.}$] from the central part of the original cylinder. The samples were vacuum-saturated and placed in a rubber sleeve. The top portion of the sleeve is used to create a reservoir where 0.3 M NaOH is placed in contact with the upper surface of the sample. The bottom of the sample is placed in a solution of 10% NaCl. The test is illustrated in

Table 1
Mixture proportions of the mortars used in this study.

Mortar mixture	0.42–0%	0.30–0%	0.30–40%	0.30–60%	0.30–40%-L	0.30–60%-L
Cement (kg/m^3)	612	731	453	307	453	307
Fly ash (kg/m^3)	–	–	252	384	252	384
Water (kg/m^3)	257	219	211	207	211	207
Water for IC (kg/m^3)	–	–	–	–	38	37
Fine aggregate (SSD) (kg/m^3)	1418	1418	1418	1418	998	1006
Oven dry LWA (kg/m^3)	–	–	–	–	236	232
HRWRA (g/100 g) cementitious material	–	0.5	0.2	0.1	0.2	0.1
Fly ash (%) (by volume)	–	–	40	60	40	60
Water/cementitious material (w/cm)	0.42	0.30	0.30	0.30	0.30	0.30
Equivalent w/c	0.42	0.30	0.47	0.67	0.47	0.67
Volume fraction of aggregate (%)	55	55	55	55	55	55

1 $\text{kg/m}^3 = 1.69 \text{ lb/yd}^3$.

“L” stands for LWA and identifies the internally-cured mortars.

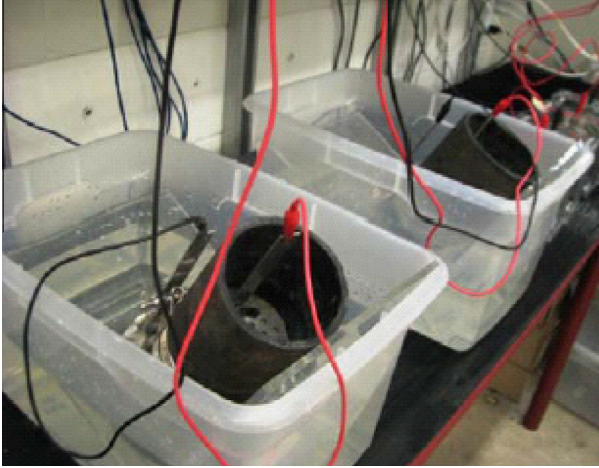


Fig. 1. Rapid chloride migration (RCM) experimental set-up.

Fig. 1. An initial electrical potential of 30 V is applied to the specimen. This potential is adjusted according to the current response (as outlined in the NT Build standard) [19] and the applied potential is maintained for a 24 h period.

At the end of the 24 h time period in which voltage was applied, the sample was rinsed with distilled water and the surface was wiped with a cloth. The sample was then split into two pieces as shown in Fig. 2. A 0.1 mol/L silver nitrate solution is sprayed on the fractured surface of the sample. Where sufficient chloride is present, the silver nitrate causes white silver chloride to precipitate as shown in Fig. 2. The chloride penetration depth is measured at 10 locations across the section and used to determine an average depth of penetration.

The chloride non-steady state migration coefficient (D_{nssm}) was calculated using Eq. (1) [21].

$$D_{nssm} = \frac{0.0239(273 + T) \cdot L}{(U - 2) \cdot t} \cdot \left(x_d - 0.0238 \sqrt{\frac{(273 + T) \cdot L \cdot x_d}{U - 2}} \right) \quad (1)$$

where D_{nssm} is the non-steady state migration coefficient ($\times 10^{-12} \text{ m}^2/\text{s}$), U is the absolute value of the applied voltage (V), T is the average value of the initial and final temperatures in the solution ($^{\circ}\text{C}$), L is the thickness of the specimen (mm), x_d is average value of the average chloride penetration depth (mm) and t is the test duration (h). A single specimen was tested for each mortar



Fig. 2. A sample from the rapid chloride migration (RCM) test that was split and sprayed with silver nitrate (AgNO_3).

mixture at each testing age, with a coefficient of variation of 9% according to NT Build 492.

3.2. Rapid chloride penetration test (RCPT)

ASTM C 1202 (or AASHTO T277) was performed on cylindrical samples with diameter of 102 mm [4 in.] and length of 204 mm [8 in.]. The day after casting, the samples were demolded, sealed in double plastic bags and stored at $(23 \pm 0.5) ^{\circ}\text{C}$ [$(73.4 \pm 0.8) ^{\circ}\text{F}$] until their testing age was reached.

At the time of testing, a disk was cut from the center of the cylinder that was $102 \pm 2 \text{ mm}$ [$4 \pm 0.08 \text{ in.}$] in diameter and $51 \pm 2 \text{ mm}$ [$2 \pm 0.08 \text{ in.}$] long. The disk was taken from the same cylinder that was prepared for the RCM test described above. A single specimen was tested for each mortar mixture at each testing age, with a coefficient of variation of 12.3% according to ASTM C1202. Prior to testing, each sample was vacuum saturated. During the test, one surface of the sample was exposed to sodium chloride solution (3% NaCl) and the other surface was exposed to sodium hydroxide solution (0.3 mol/L NaOH). A 60 V external potential was applied and the current at 5 min intervals was recorded for a 6 h period. Fig. 3 shows the experimental set up with four samples being tested simultaneously.

Alternative interpretations of this test have been proposed, namely that the resistance after a short duration test (usually 1 min or 5 min) be used to calculate the resistivity [22–24].

3.3. Apparent chloride diffusion coefficient

Based on ASTM C1543, 102 mm [4 in.] by 102 mm [4 in.] cylinders were prepared from four of the mortar mixtures shown in Table 1: 0.42–0%, 0.30–0%, 0.30–60%, and 0.30–60%–L. Two specimens were tested for each mortar mixture at each testing age. The specimens were sealed-cured for 28 d, and then dried at 50% RH and $(23 \pm 0.5) ^{\circ}\text{C}$ [$(73.4 \pm 0.8) ^{\circ}\text{F}$] for an additional 28 d. After this time period an epoxy was used to seal the sides of the cylinders to prevent evaporation during the test and to impose uni-directional control of the chloride penetration. The chlorides came from a salt solution (3% NaCl) poured on top of the cylinders and held in place by a dike attached to the cylinder. A cover was placed on the top to avoid evaporation of the salt solution during the following ponding periods:

- 3, 6 months (after specified curing period).
- 3, 6 months after 1 year sealed-curing.

Although this test allows for uni-directional chloride penetration, the method of conditioning the samples may have induced some initial absorption, so it is not a pure diffusion test. In addition, the exposure of the bottom face to a 50% RH environment

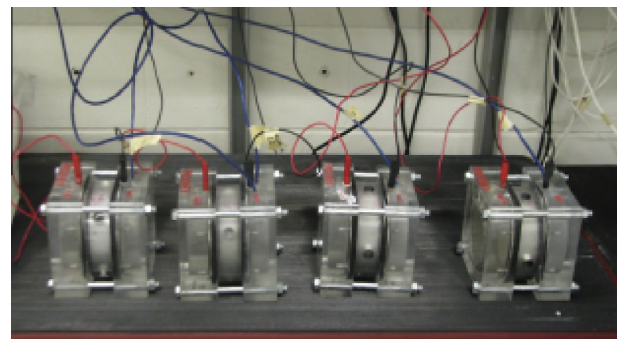


Fig. 3. Rapid chloride penetration test (RCPT) cells.

during the test induces evaporation at that surface, meaning that chlorides can also migrate by wicking action.

After each ponding period was over, the samples were ground in layers of 1 mm so that the powder could be analyzed in terms of its total chloride content by titration. Chloride penetration profiles were assessed and apparent chloride diffusion coefficients were estimated based on Fick's Second Law, as shown in the following equation

$$\frac{C_x - C_o}{C_s - C_o} = 1 - \operatorname{erf}\left(\frac{x}{\sqrt{4 \cdot D_a \cdot t}}\right) \quad (2)$$

where C_x (%) is the chloride concentration at any point x (m) at any time t (s), C_o is the background chloride concentration (%), C_s is the surface chloride concentration (%), D_a is the apparent chloride diffusion coefficient (10^{-12} m²/s), and erf is the error function.

3.4. Surface resistivity

The electrical resistivity was also measured using cylindrical samples that were 102 mm [4 in.] in diameter and 204 mm [8 in.] long and cured in lime water, using the four-point Wenner probe surface testing device (i.e. Wenner, see Fig. 4), as described in AASHTO TP 95-11. Three specimens were tested for each mortar mixture at each testing age.

In this test, current is applied at the outer probes and the potential difference is measured between the two inner probes. Assuming that the sample has homogeneous semi-infinite geometry, the mortar resistivity is described by Eq. (3) [25]:

$$\rho = R \cdot k \quad (3)$$

where R is the measured resistance (Ω), and k is the geometry correction shown in Eq. (4) based upon a fit of the data presented by Morris et al. [26].

$$k = \frac{2\pi a}{1.10 - \frac{0.730}{\frac{d}{a}} + \frac{7.82}{\left(\frac{d}{a}\right)^2}} \quad (4)$$

This approximation is only valid for cylindrical specimens with $d/a \leq 4.0$ and $L/a \geq 5.0$, where d is the diameter of the cylinder, a is the interprobe distance of the Wenner apparatus, and L is the length of the cylinder.

Pore solution extraction was also conducted at different ages: 10 min and every one hour while still in the fresh state by a Millipore pressure filtering system, using nitrogen gas at pressures up to 200 kPa. The procedure has been previously used and described in [27]. Extractions performed on hardened samples were conducted at ages of 1 d and 3 d using a high pressure die at pressures up to 380 MPa, as described by Barneyback et al. [28].

After extraction, pore solution resistance was measured at different ages. This was done through the use of a conductivity cell, with stainless steel electrodes at the ends of a short polycarbonate tube. The geometry factor of 0.212 cm of the cell was determined using the ratio of area to length and was confirmed using a solution of known conductivity.

Using a Solatron 1260 Impedance Gain-Phase analyzer with a frequency range of 1 MHz to 10 Hz, and a 500 mV AC Signal, the measured resistance was obtained and corrected by the geometry factor according to Eq. (3) to obtain the electrical resistivity.

3.5. Water absorption

The amount of water absorbed and the rate at which water is absorbed (referred to as sorptivity) can provide useful information concerning pore connectivity and pore volume, both of which are important in evaluating the durability of cementitious materials.

Replicate 102 mm \times 204 mm [4 \times 8 in.] cylinders were prepared from each mortar mixture in Table 1. Each cylinder was cast, demolded at 24 h, and sealed in a double layer of plastic bags. Two cylinders were cast for each testing age of 28 d or 90 d. After each curing age, one of the two cylinders was demolded and three 51 \pm 2 mm [2 \pm 0.08 in.] thick specimens were cut from the central portion of the cylinder. The specimens were then placed in an isothermal (23 \pm 0.5) $^{\circ}$ C [(73.4 \pm 0.8) $^{\circ}$ F] environment at 65 \pm 1% RH until they reached mass equilibrium, defined as less than a 0.02% in mass over a period of 15 d. This conditioning method lasted approximately 1 year and was chosen to provide consistent moisture content in all of the samples [29,30].

Prior to absorption testing, the side surface of the samples was sealed with aluminum tape and the top surface was covered with plastic wrap. This was to prevent drying of the sample from these surfaces. Other researchers [29] have used epoxy rather than aluminum tape as the test was carried out for longer ages (i.e., 1 year). The remainder of the procedure was conducted in accordance with ASTM C1585-11.

The amount of absorbed water is normalized by the cross-section area of the specimen exposed to the fluid using Eq. (5):

$$i = \frac{m_t}{a \cdot \rho} \quad (5)$$

where i is the normalized absorbed fluid volume (mm³/mm²), m_t is the specimen mass at time t (g); a is the area of the specimen exposed to the fluid (i.e., that of the bottom face) (mm²), and ρ is the density of the absorbed fluid (taken to be 0.001 g/mm³ at 23 $^{\circ}$ C for water).



Fig. 4. Wenner probe surface testing device. Certain commercial products are identified in this paper to specify the materials used and procedures employed. In no case does such identification imply endorsement or recommendation by the National Institute of Standards and Technology, EMPA, Purdue University or Universidad del Desarrollo, nor does it indicate that the products are necessarily the best available for the purpose.

The absorbed fluid volumes are then plotted as a function of the square root of time. The initial sorptivity is determined from the slope of the curve during the first 6 h according to ASTM C1585-11, while secondary sorptivity is determined using the slope of the same measurements between 1 d and 8 d, as outlined in ASTM C1585. The initial and secondary sorptivities can be used to evaluate the connectivity of the pore network [29].

4. Results and discussion

4.1. Chloride transport tests

The measured non-steady state migration chloride coefficients from four of the mortar mixtures are provided in Table 2. The 0.42–0% mortar had the greatest values of diffusion coefficients at all ages. While at early ages, the diffusion coefficients for the 0.30–0%, 0.30–60%, and 0.30–60%-L mortars are comparable, it is evident that at later ages (after 1 year) the diffusion coefficient decreases significantly in both fly ash mortars. The reduction in the diffusion coefficient of the HVFA mixtures over time suggests that there is plenty of curing water available in these systems (just provided from the mix water). In other words, the equivalent w/c of these mixtures would correspond to a $w/c = 0.67$, allowing the achievement of higher degrees of hydration, thereby reducing the diffusion coefficient.

It should be noted that the bulk diffusion coefficients of actual in-place concrete may actually be lower than the values shown for the internally-cured mortar. First, the internally cured mortar is cut to perform the test. As such, the cutting of the concrete exposes porous lightweight aggregate surfaces. When these cut aggregates are exposed to the solution, the chloride can easily diffuse/absorb quickly into the exposed LWA portions of the mortar which may not represent what happens in field concretes where the LWA are not exposed. As such, these results represent conservative estimates for the diffusion coefficient. In addition, since the sample was vacuum-saturated, the conductivity of the lightweight aggregate may alter the electrical response of the concrete [31].

Similarly, the results from the RCPT for the same four mortar mixtures are shown in Table 3. It is worthwhile to mention that the charge passed values shown in Table 3 are much higher than what is typically reported in concretes mixtures (for instance, values larger than 4000 coulombs are considered to yield into high chloride ion penetrability by ASTM C1202). This is because the results shown in Table 3 were obtained in mortars with only 55% aggregates volume. As it can be observed, the charge passed

Table 2
Chloride diffusion coefficients obtained from the rapid chloride migration test.

Time (d)	Diffusion coefficients ($10^{-12} \text{ m}^2/\text{s}$)			
	0.42–0%	0.30–0%	0.30–60%	0.30–60%-L
28	13.8	3.68	5.54	3.49
56	18.2	4.58	2.46	3.97
91	13.9	4.40	1.41	2.03
365	7.94	2.25	0.29	0.48

Table 3
Rapid chloride penetration test results for the mortars samples.

Time (d)	Charge passed (C)			
	0.42–0%	0.30–0%	0.30–60%	0.30–60%-L
28	*	14,026	3137	4398
56	15,263	8894	2167	*
365	5083	1061	129	114

* Test not performed.

decreases over time in all mortar mixtures, which is attributed to increased hydration. In other words, more hydration products are formed, thus decreasing the number of interconnected pores of the samples. When comparing the two plain mortars (0.42–0% and 0.30–0%), it is evident that less charge will pass through the lower w/c mortar (42% and 79% less at 56 d and 365 d respectively). Both HVFA mortars also show lower charge passed values throughout the testing ages compared to the control 0.42–0% and 0.30–0% mixtures.

The use of the RCPT method can be thought of essentially as a measure of concrete resistivity. However, it should be noted that RCPT was performed with high voltage and the samples heated during testing, which increases the charge passes due to the Joule effect. As such, there is no need to continue the test for 6 h, and changes in the current during this time are most likely due to increases in temperature, not chloride penetration [24,32]. It is also important to emphasize that even though it is well known that the use of supplementary cementitious materials will improve the pore structure reducing the penetrability, on the other hand, they are also able to modify the chemistry of the pore solution. As a consequence, any change in the alkalinity of the system due to the mineral admixtures may result in misleading values.

The lower chloride diffusion coefficients obtained in the HVFA mixtures (both IC and non-IC) are translated into less chloride penetration from the concrete surface compared to the control 0.42–0% mixture at all different curing/ponding time periods used in this study. This is observed in Fig. 5. However, the internally cured HVFA mixture shows larger amounts of chloride within the first 3 mm to 4 mm (this makes sense since the LWA used consisted of fine particles with a nominal maximum size of 4.76 mm). Other studies have attributed this effect to the fact that the top surface of the samples are cut, thereby exposing the pores of the LWA at the surface of the sample. The exposed LWA pores are much larger than the paste pores. As a consequence, LWA pores can work as reservoirs for the chloride solution which can be easily absorbed and rapidly diffuse into the LWA pores.

The apparent chloride diffusion coefficients can be calculated using these profiles and Eq. (2). They are provided in Table 4. It can be observed how the apparent chloride diffusion coefficient decreases when the samples were cured for an additional year, increasing their degree of hydration and, therefore, decreasing the chloride penetration. This is observed in all four mixtures. While the 0.42–0% mortar shows higher values of apparent diffusion coefficients compared to the other mixtures, both HVFA mixtures show similar results between them, but still lower values than the 0.30–0% mortar. Therefore, an improvement in transport properties is observed in the HVFA mixtures if compared to either the 0.42–0% or 0.30–0% mortars.

4.2. Electrical tests

Fig. 6 shows the “normalized” surface resistivity measurements for four of the mortars described in Table 1. The mortars were stored in lime water so they can be considered to be close to saturation. The normalization is performed by dividing the bulk surface resistivity by the pore solution resistivity at the different ages shown in Fig. 6 (1 d, 3 d, 7 d, 14 d, 28 d, 56 d, 91 d, and 365 d). This corresponds to plotting the formation factor, as explained in Eq. (6). The formation factor characterizes the solid microstructure and it is directly related to the transport properties of a porous medium [33].

$$F = \frac{\rho_t}{\rho_o} \quad (6)$$

where F is the formation factor, ρ_t is the mortar resistivity ($\Omega \text{ m}$), and ρ_o is the pore solution resistivity ($\Omega \text{ m}$).

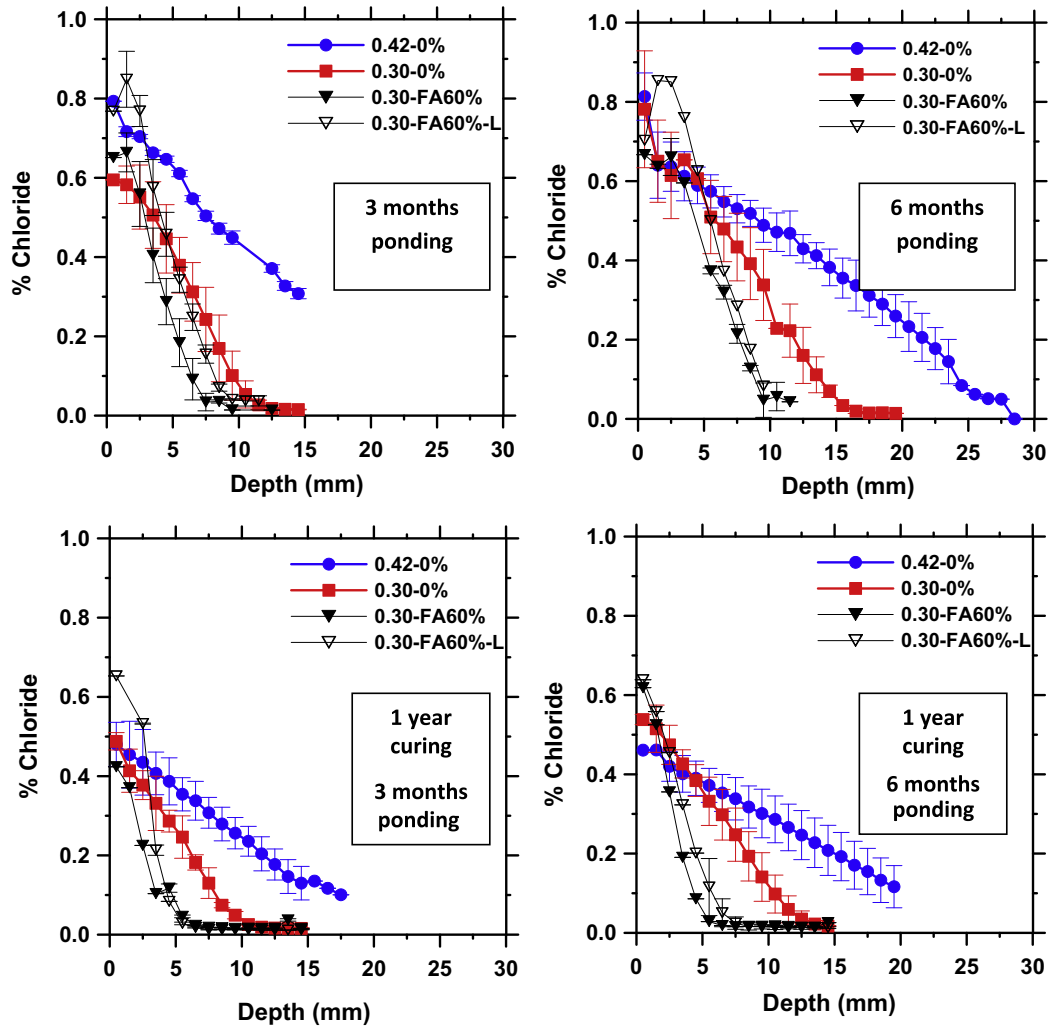


Fig. 5. Chloride penetration profiles at different curing/ponding time periods (error bars represent the standard deviation from the average of three samples).

Table 4

Apparent chloride diffusion coefficients approximated using Fick's 2nd Law (numbers in parentheses represent the standard deviation of two samples).

Time (d)	Apparent diffusion coefficients ($10^{-12} \text{ m}^2/\text{s}$)			
	0.42-0%	0.30-0%	0.30-60%	0.30-60%-L
91 (Ponding)	17.6 (0.3)	3.47 (0.5)	1.12 (0.1)	1.75 (0.1)
180 (Ponding)	11.6 (0.7)	3.19 (0.5)	1.10 (0.1)	0.94 (0.1)
365 (Curing) + 91 (ponding)	12.1 (0.8)	2.65 (0.4)	0.72 (0.1)	0.89 (0.1)
365 (Curing) + 180 (ponding)	10.6 (0.9)	2.10 (0.4)	0.32 (0.1)	0.61 (0.1)

However, after 7 d, pore solutions extractions are difficult to perform since the amount of liquid in the samples is low. Instead, an extrapolation from the pore solution resistivity vs. degree of hydration (DOH) curve was performed. These two parameters are linearly related after a certain degree of hydration [25]. Estimating the DOH at the different ages mentioned above, it was then possible to calculate the pore solution resistivity, and thus, normalize the results in Fig. 6. However, the resistivity values obtained from sealed-cured specimens do not correspond to values from samples that have been saturated. Thus, an additional correction for this must be performed. The approach taken was to calculate the sealed-to-saturated pore solution resistivity ratio using a model developed at NIST [34], that can estimate the pore solution resistivity in both conditions (i.e., sealed and saturated). The tested (sealed) pore solution resistivity was then corrected to saturated conditions with that factor for each mortar mixture.

As observed in Fig. 6, the HVFA specimens have similar resistivity values to that of the 0.42-0% mortar at 91 d, and keep increasing over time, even surpassing the 0.30-0% mortar at about 300 d of hydration. After 1 year, both HVFA mixtures reach resistivity values up to 3 times larger than those obtained by the 0.42-0% mortar.

4.3. Water absorption test

Fig. 7 shows the absorbed water throughout the 8 d of testing as a function of the square-root of time. It is observed that there is a decrease in the amount of absorbed water when the samples were cured during 28 d and 90 d before drying. This happens in all the samples prepared and it is attributed to the higher degree of hydration reached, thus decreasing the capillary porosity and the amount of absorbed water. Fig. 7(a) and (b) show the comparison

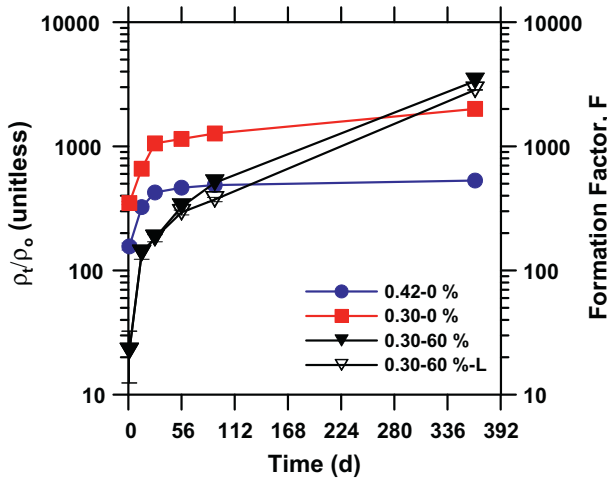


Fig. 6. Formation factor as a function of time of mortars samples stored in lime water up to 365 d (error bars represent the standard deviation from the average of three samples).

of the 0.42–0% mortar with the HVFA mortars. It can be noticed that, after 8 d of testing, the 0.42–0% mortar absorbs approximately three times more water than the low w/cm HVFA mortars, which is in agreement with the fact that a higher volume of larger pores would be present in the high w/c mortar.

When analyzing the effect that IC has on the HVFA mortars (Fig. 7(c) and (d)), it can be observed that, while the IC mortars absorbed between 25% and 50% more water than the non-IC HVFA mortars at 28 d, there is a decrease of 25% in the amount of water absorbed in the IC samples cured for 90 d. It is important to remember at this point that the IC-HVFA mortars are intended to replace the 0.42–0% (reference mixture corresponding to a typical bridge deck concrete mix). The IC-HVFA mortars cured for 90 d have a similar performance in terms of water absorption as a plain 0.30 mixture. This would positively influence the durability of the material.

Fig. 8(a) and (b) show the initial sorptivities calculated as the slope of the absorption vs. the square root of time during the first 6 h of testing. Initial sorptivity of the 0.42–0% mortar is approximately 4 times higher than the 0.30–0% mortar. The inclusion of fly ash in the low w/cm mortar does decrease the rate of water absorption in comparison with the 0.42–0% mortar as well. The

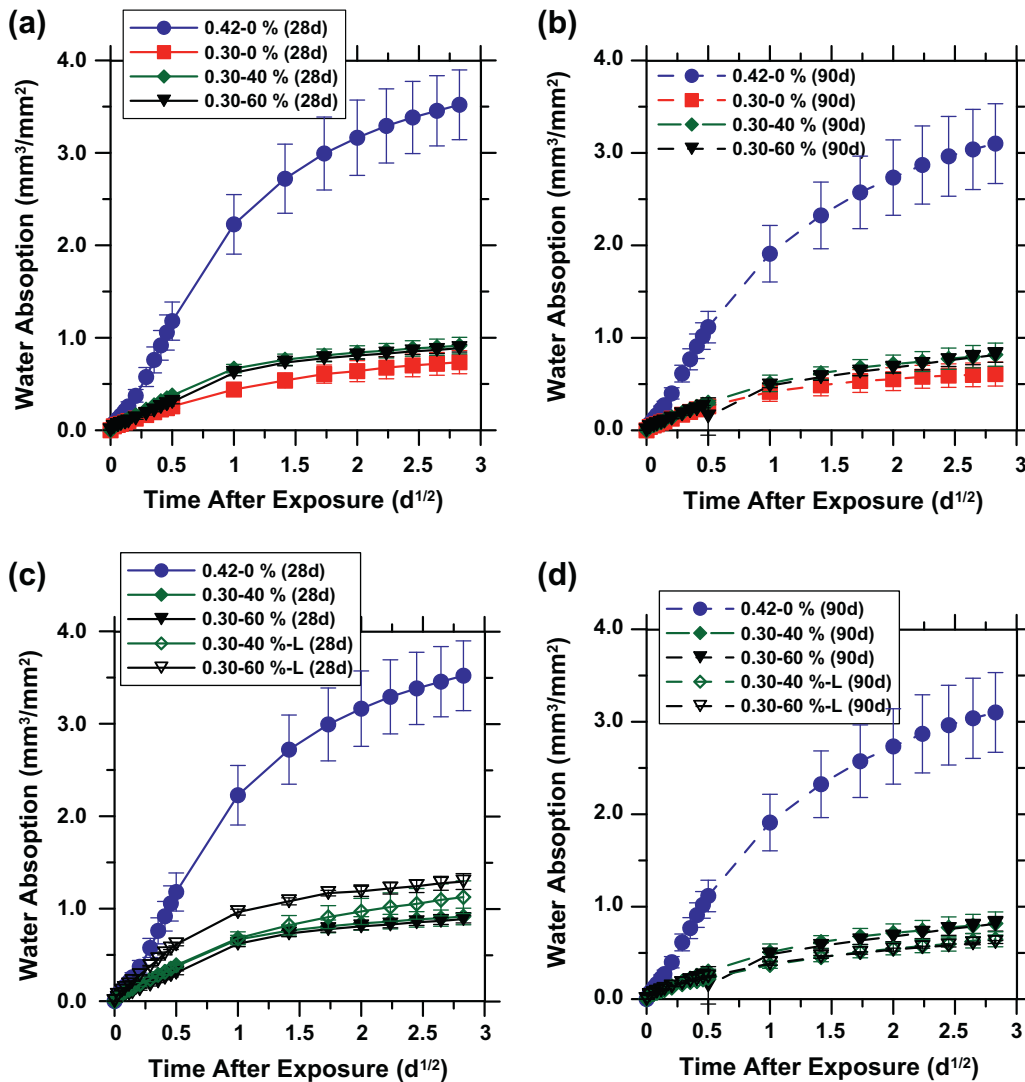


Fig. 7. Absorbed water of sealed-cured mortars samples (a) as a function of fly ash content curing during 28 d, (b) as a function of fly ash content curing during 90 d, (c) including IC and curing 28 d, (d) including IC and curing 90 d (error bars represent the standard deviation from the average of three samples).

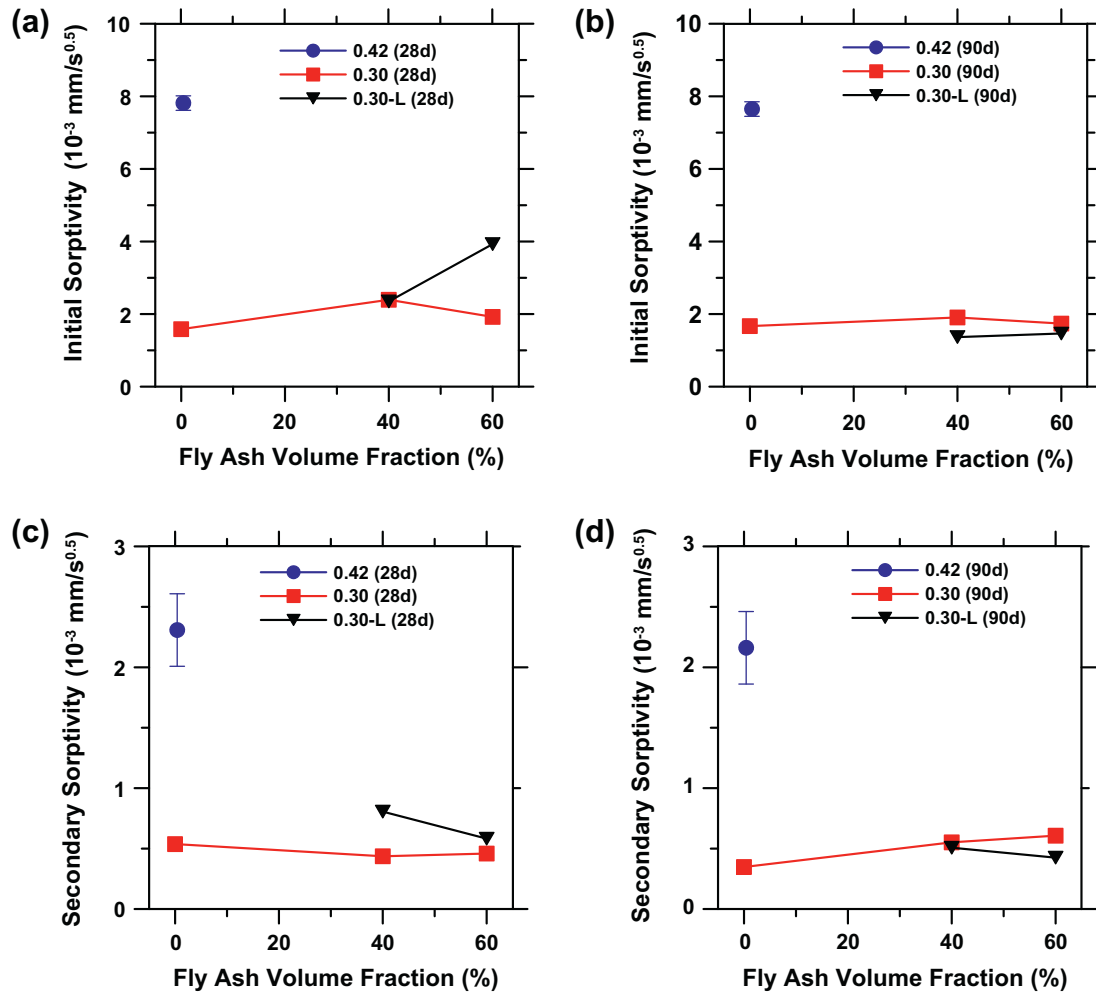


Fig. 8. (a and b) Initial sorptivity of the sealed-cured mortars samples, (c and d) secondary sorptivity of the sealed-cured mortars samples.

inclusion of IC does not reduce the amount of water absorbed at 28 d, being the same for the 40% fly ash mortar, and higher for the 60% fly ash mortar. However, IC slightly decreases the absorption rate at later ages (e.g., 90 d) in the HVFA mortars, which is attributed to a further hydration.

Fig. 8(c) and (d) show the secondary sorptivity calculated as the slope of the absorption vs. the square root of time between 1 d and 8 d of testing. Trends are similar to those obtained for the initial sorptivity. Internally cured HVFA mixtures absorb a much lower amount of water and at a slower rate than a mortar with a w/c of 0.42.

The water absorption results must be carefully interpreted when LWA are included in the mixtures, as they can act as empty water reservoirs. This might be more relevant at early ages, especially when samples have been exposed to a drying environment (i.e., $65 \pm 1\%$ RH), as indicated in the conditioning method used for the water absorption test [29]. At 28 d, it may be possible that the water contained in the LWA particles in the high volume fly ash mixtures is not completely consumed by the cement reaction; thereby, the degree of hydration is not high enough to achieve capillary pore depercolation within the cement paste matrix. As such, when samples are dried, water in LWA may evaporate, but leaving behind a path for water to re-ingress during a subsequent absorption test. At later ages (e.g., 90 d), a higher degree of hydration is achieved, densifying the cement paste matrix and, therefore, isolating the LWA particles within the cement paste matrix. In this

case, the LWA particles will not be easily accessible for water to re-ingress during the absorption test, even after the sample has been dried.

5. Summary and conclusions

This paper is the second paper in a series investigating the performance of HVFA mixtures with low w/c that are internally cured. The low w/cm HVFA mixtures with and without IC have been compared to a typical w/c (i.e., 0.42) used in concrete transportation structures (e.g., bridge deck). The study has demonstrated the benefits of using IC in low w/cm HVFA mixtures in reducing fluid transport by performing various transport tests on mortar mixtures. The following conclusions can be drawn:

- Chloride diffusion is considerably reduced in low w/cm HVFA mixtures (with or without IC) compared to a control w/c = 0.42 mixture. However, the chloride penetration within the first 3–4 mm from the top surface of a specimen cut from a cast cylinder is larger in the IC HVFA mortars due to the surface exposure of porous LWA. This effect has been reported elsewhere [31] and must be considered when evaluating transport properties in internally cured mixtures.
- Electrical measurements (i.e., surface resistivity) indicate that the low w/cm HVFA mixtures have similar resistivity values as the control 0.42–0% mortar at 91 d, but improve over time. After

1 year, both HVFA mixtures reach resistivity values up to 3 times larger than those obtained by the 0.42–0% mortar. This is attributed to denser microstructure achieved in the HVFA specimens (both IC and non-IC).

- The amount and rate of water absorbed in HVFA samples with and without IC is considerably reduced compared to a control $w/c = 0.42$ mortar.

In conclusion, while the transport properties of low w/cm HVFA mixtures (with or without IC) are considerably reduced compared to a control $w/c = 0.42$ mixture, IC does not really provide a further reduction of the fluid and ion transport in concrete with similar cementitious content. However, IC provides benefits in increased strength and reduced cracking as indicated in a previous study [5], without detrimentally impacting transport properties, which are likely controlled first and foremost by the high level of replacement of cement with fly ash and the pore refinement/increased alkali sorption that such replacement provides. Nevertheless, and from a practical perspective, if low w/cm HVFA with IC mixtures substitute a typical $w/c = 0.42$ bridge deck concrete, the reduction in fluid transport would be considerable, thus improving the durability of the steel reinforced concrete used in structural elements.

References

- [1] ACI 232.2R-03. Use of fly ash in concrete. Farmington Hills, MI: American Concrete Institute; 2003.
- [2] Obla K, Lobo C, Kim H. Greatly increased use of fly ash in hydraulic cement concrete (HCC) for pavement layers and transportation structures – volume I. Final report, NRMCA; 2012.
- [3] Malhotra VM, Mehta PK. High performance, high-volume fly ash concrete. Ottawa, Canada: Supplementary Cementing Materials for Sustainable Development Inc.; 2005.
- [4] Malhotra V. Durability of concrete incorporating high-volume of low calcium (ASTM Class F) fly ash. *Cem Concr Compos* 1990;12(4):271–7.
- [5] De la Varga I, Castro J, Bentz DP, Weiss J. Internal curing concepts in mixtures containing high volumes of fly ash. *Cem Concr Compos* 2012;34(9):1001–8.
- [6] Pease B, Hossain AB, Weiss J. Quantifying volume change, stress development, and cracking due to early-age autogenous shrinkage. *ACI Special Publ March* 2004;220:23–39.
- [7] Bentz DP, Weiss J. Internal curing: a 2010 state of the art review. NISTIR 7765. Gaithersburg, MD: National Institute of Standards and Technology, US Department of Commerce; 2011.
- [8] Philleo R. Concrete science and reality. In: Skalny JP, Mindess S (editors), *Materials Science of Concrete II*. Westerville OH: American Ceramic Society; 1991.
- [9] EuroLightCon. LWAC material properties state-of-the-art. In: *Economic design and construction with light weight aggregate concrete*. Brite-EuRam III; 1998. p. 47–8.
- [10] Castro J. Moisture transport in cement based materials: applications to transport test and internal curing. PhD dissertation. West Lafayette, Indiana: Purdue University; 2011.
- [11] Bentz DP. Influence of internal curing using lightweight aggregates on interfacial transition zone percolation and chloride ingress in mortars. *Cem Concr Compos* 2009;31(5):285–9.
- [12] Delagrave A, Bigas JP, Ollivier JP, Marchand J, Pigeon M. Influence of the interfacial zone on the chloride diffusivity of mortars. *Adv Cem Mater* 1997;5(3–4):86–92.
- [13] Peled A, Castro J, Weiss J. Atomic force microscopy examinations of mortar made by using water-filled lightweight aggregate. *Journal of the transportation research board*, No. 2141. Washington, DC: Transportation Research Board of the National Academies; 2010. p. 92–101.
- [14] Bentz DP, Stutzman PE. Internal curing and microstructure of high performance mortars. ACI SP-256. In: Bentz D, Mohr B, (editors), *Internal curing of high performance concretes: laboratory and field experiences*; 2008. p. 81–90.
- [15] Castro J, Keiser L, Golias M, Weiss J. Absorption and desorption properties of fine lightweight aggregate for application to internally cured concrete mixtures. *Cem Concr Compos* 2011;33(10):1001–8.
- [16] NYDOT. Test method No.: NY 703-19 E. Moisture content of lightweight fine aggregate. Albany, NY: New York State Department of Transportation, Materials Bureau; August 2008.
- [17] Kantro DL. Influence of water-reducing admixtures on properties of cement paste-a miniature slump test. *Cem. Concr, Aggreg* 1980;2:95–102.
- [18] Golias M, Bentz D, Weiss J. Influence of exposure conditions on the efficacy of internal curing. *Adv Civil Eng Mater* 2012.
- [19] NT Build 492. Chloride migration coefficient from non-steady-state migration experiments, Nordtest method.
- [20] Hooton D, Nagi MA, Ozyildirim HC. The rapid chloride permeability test. *HPC Bridge Views* 2000(12):2–4. November/December.
- [21] Tang L. Chloride diffusion coefficient of concrete and relevant test methods: the state-of-the art and suggestions for future work. Swedish National Testing and Research Institute; 1997.
- [22] Riding KA, Poole JL, Schindler AK, Juenger MCG, Folliard KJ. Simplified concrete resistivity and rapid chloride permeability test method. *ACI Mater J* 2008;105:390–4.
- [23] ASTM C1760-12. Standard test method for bulk electrical conductivity of hardened concrete. West Conshohocken, PA: ASTM International; 2012.
- [24] Snyder KA, Ferraris C, Martys NS, Garboczi EJ. Using impedance spectroscopy to assess the viability of the rapid chloride test for determining concrete conductivity. *J Res Natl Inst Stand Technol* 2000;105:497–509.
- [25] Spragg R, Villani C, Snyder K, Bentz D, Bullard J, Weiss WJ. Electrical resistivity measurements in cementitious systems: observations of factors that influence the measurements. Accepted for TRB 91st annual meeting compendium of papers. Washington, DC: Transportation Research Board; 2013.
- [26] Morris W, Moreno EI, Sagues AA. Practical evaluation of resistivity of concrete in test cylinders using a Wenner array probe. *Cem Concr Res* 1996;26:1779–87.
- [27] Penko M. Some early hydration processes in cement paste as monitored by liquid phase composition measurements. PhD dissertation. West Lafayette, Indiana: Purdue University; 1983.
- [28] Barneyback RS, Diamond S. Expression analysis of pore fluids from hardened cement pastes and mortars. *Cem Concr Res* 1981;11:279–85.
- [29] Castro J, Bentz D, Weiss J. Effect of sample conditioning on the water absorption of concrete. *Cem Concr Compos* 2011;33(10):805–13.
- [30] Golias M, Castro J, Weiss J. The influence of the initial moisture content in lightweight aggregate on internal curing. *Constr Build Mater* 2012;35:55–62.
- [31] Weiss J, Bullard J, Snyder K, Bentz D, Castro J. Electrical properties of concrete with conductive aggregate: implications for internal curing. *Work Prep* 2013.
- [32] Betancourt GA, Hooton RD. Study of the Joule effect on rapid chloride permeability values and evaluation of related electrical properties of concretes. *Cem Concr Res* 2004;34:1007–15.
- [33] Snyder K. The relationship between the formation factor and the diffusion coefficient of porous materials saturated with concentrated electrolytes: theoretical and experimental considerations. *Concr Sci Eng* 2001;3(12):216–24.
- [34] <http://concrete.nist.gov/poresolnalc.html>, access verified April 2013.